European Spine Journal (2019) 28:1724–1732
https://doi.org/10.1007/s00586-019-06006-0

ORIGINAL ARTICLE

Evaluation of iliac screw, S2 alar-iliac screw and laterally placed triangular titanium implants for sacropelvic fixation in combination with posterior lumbar instrumentation: a finite element study

Gloria Casaroli[1] · Fabio Galbusera[1] · Ruchi Chande[2] · Derek Lindsey[2] · Ali Mesiwala[3] · Scott Yerby[2] · Marco Brayda-Bruno[1]

Received: 17 January 2019 / Revised: 10 April 2019 / Accepted: 9 May 2019 / Published online: 15 May 2019

Abstract

Purpose This study aimed to implement laterally placed triangular titanium implants as a technique of sacropelvic fixation in long posterior lumbar instrumentation and to characterize the effects of iliac screws, S2 alar-iliac screws and of triangular implants on rod and S1 pedicle screw stresses.

Methods Four female models of the lumbopelvic spine were created. For each of them, five finite element models replicating the following configurations were generated: intact, posterior fixation with pedicle screws to S1 (PED), with PED and iliac screws (IL), with PED and S2 alar-iliac (S2AI) screws, and with PED and bilateral triangular titanium implants (SI). Simulations were conducted in compression, flexion–extension, lateral bending and axial rotation. Rod stresses in the L5-S1 segment as well as in the S1 pedicle screws were compared.

Results One anatomical model was not simulated due to dysmorphia of the sacroiliac joints. PED resulted in the highest implant stresses. Values up to 337 MPa in lateral bending were noted, which were more than double than the other configurations. When compared with IL, S2AI and SI resulted in lower stresses in both screws and rods (on average 33% and 41% for S2AI and 17% and 50% for SI).

Conclusions Implant stresses after S2AI and SI fixations were lower than those attributable to IL. Therefore, pedicle screws and rods may have a lower risk of mechanical failure when coupled with sacropelvic fixation via S2AI or triangular titanium implants, although the risk of clinical loosening remains an area of further investigation.

Graphical abstract

These slides can be retrieved under Electronic Supplementary Material.

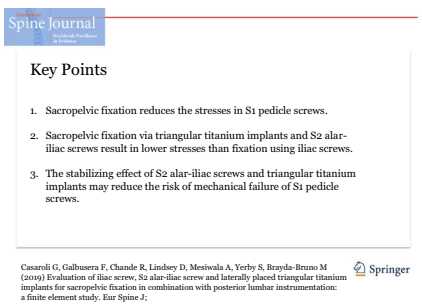

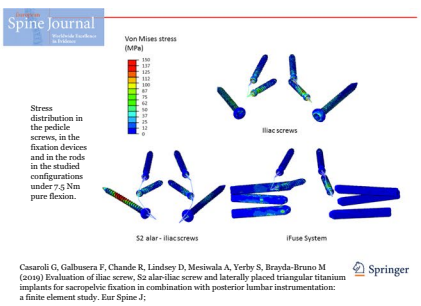

Electronic supplementary material The online version of this article (https://doi.org/10.1007/s00586-019-06006-0) contains supplementary material, which is available to authorized users.

Extended author information available on the last page of the article

Keywords Sacroiliac joint · Sacropelvic fixation · Finite element analysis · Alar-iliac screws · Iliac screws · Triangular implants

Introduction

In select cases of complex spinal deformity correction, sacropelvic fixation is necessary to provide stability to the posterior lumbosacral construct, especially when the L5-S1 level is instrumented [1]. Indeed, poor sacral bone quality and high loads acting at the lumbosacral segment favor screw loosening and implant failure and increase the risk of developing pseudoarthrosis at L5-S1 [2–5]. Modern techniques commonly used in sacropelvic fixation are iliac screws and S2 alar-iliac screws [2]. Several in vitro studies have demonstrated a similar improvement in the construct stability and a decrease in the strain in S1 pedicle screws, which are the most susceptible to failure and loosening [6–8].

Clinical studies reported marked differences between the outcomes of sacropelvic fixation with either iliac or S2 alar-iliac screws. Although follow-up studies reported a decrease in the rate of L5-S1 pseudoarthrosis from 9 to 3% of cases due to iliac screws fixation [9, 10], it was found that 20% of patients had unsuccessful outcomes due to the pain caused by prominent hardware, loosening of iliac or S1 pedicle screws, or mechanical failure of the connectors [2]. Moreover, the infection rates reported for long fixations in adult deformity surgeries have been associated, at least to some extent, to the additional surgical exposure required for pelvic fixation with iliac screws [2]. Compared to iliac screws, S2 alar-iliac screws have several advantages. First, the medial position allows linkage to the rods without the need for additional connectors [2]. Second, the insertion points, located more anteriorly to the lumbosacral pivot point, may improve the stability of the construct [11–13]. Third, the deep insertion point avoids the generation of the postoperative hardware pain commonly caused by iliac screws [2]. On the downside, although it was demonstrated that S2 alar-iliac screws can be safely implanted with a proper free-hand technique [14], their trajectory is close to various important neurological and vascular structures, with potential risk of perioperative complications [15]. Furthermore, they may cause increased sacroiliac pain over time [14].

Currently, the iFuse Implant System (SI-BONE Inc., Santa Clara, CA) is used to stabilize the sacroiliac joint (SIJ) in cases of sacroiliac joint disruption and degenerative sacroiliitis, through a minimally invasive procedure [16–18]. This technique, which involves laterally placing three triangular titanium implants across the SIJ, has several advantages such as less blood loss, lower surgical time and hospital stay, and more successful outcomes than traditional open surgical techniques to treat degenerative sacroiliitis and SIJ pain [16]. The iFuse Implant System consists of cannulated triangular implants made of a titanium alloy (Ti6Al4 V) with a porous surface aimed at facilitating osteointegration; the implant surface and shape are designed to minimize the motion of the SIJ. These implants have also been used on patients with symptomatic SIJ degeneration secondary to long posterior fusion with good clinical outcomes in a short and medium follow-up period [19]. Finite element studies [20, 21] investigating the use of solid triangular titanium implants have shown a decrease in the range of motion (ROM) of the SIJ up to 70, 38 and 69% in flexion–extension (FL-EX), lateral bending (LB) and axial rotation (AR), respectively.

This study sought to (1) implement triangular titanium implants, a SI joint stabilization device, as a means of sacropelvic fixation and (2) characterize and compare the effects of the triangular titanium implants, iliac screws and S2AI screws on the stresses in S1 pedicle screws and L5-S1 rods.

Materials and methods

Four female anatomical models of the lumbosacral spine were generated using in-house software. The geometries of the models were based on CT scans (Siemens SOMATOM Definition AS, 0.77 mm × 0.77 mm × 2.00 mm resolution, 140 kV voltage, 480 mA) acquired at I.R.C.C.S. Istituto Ortopedico Galeazzi (Milan, Italy) and anonymized; written informed consent for the use of the data for research purposes was previously obtained. Linear tetrahedral meshes were generated, and a convergence study with meshes of three different element dimensions was performed; the convergence analysis was based on the range of motion (ROM) of the SIJ, and a difference of less than 5% between the meshes was considered acceptable. The final models contained between 572,698–828,572 and 126,593–157,281 nodes and elements, respectively. The models included a portion of the L4 vertebra visible in the CT scan, L5, sacrum and pelvis. Anatomical measurements were taken to investigate the differences among the four patients: we measured the maximum S1 vertebral body length (S1L) and width (S1 W), the maximum sacrum length and width (SL and SW), the sacrum height (SH) as the distance between the center of the S1 endplate (S) and the inferior extremity of the coccyx, and the distance between the S and the center of the acetabulum (CS) (Fig. 1). The pelvisacral incidence (PSI) was measured as the angle identified by the line adjacent to S1 endplate and the projection of the CS segment in the sagittal plane (Fig. 1) [22].

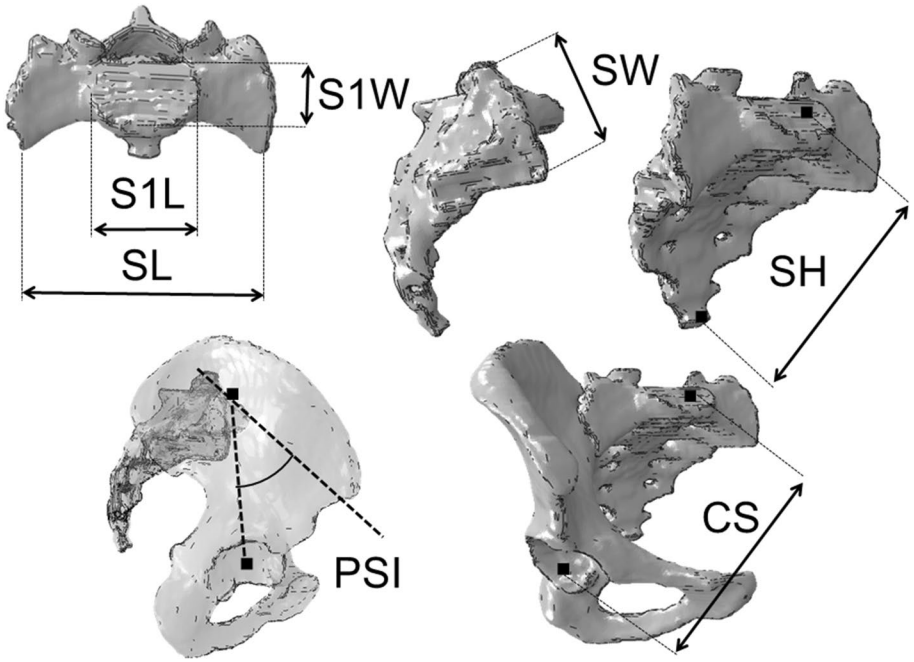

Fig. 1 Schematic representation of the anatomical measurements. S1L is S1 length, S1 W is S1 width, SL is sacrum length, SW is sacrum width, SH is sacrum height, PSI is pelvisacral incidence, CS

Bone was modeled as a linear elastic material with a Poisson ratio, υ, of 0.3 and a Young's modulus, E, ranging between 0.2 and 18 GPa based on the gray value [23]. The pelvic ligament bundles were modeled as nonlinear spring elements with stiffness properties taken from the literature (Table 1) [24–26]. Intervertebral disks were simply modeled with solid elements having a Young's modulus of 6 MPa and Poisson's ratio of 0.45 [27].

For each of the four patients, five configurations were generated: (1) intact, (2) treated with L4-S1 pedicle screws (PED), (3) treated with L4-S1 pedicle screws and iliac screws (IL), (4) treated with L4-S1 pedicle screws and bilateral alar-iliac screws in S2 (S2AI) and (5) treated with L4-S1 pedicle screws and bilateral 7.0 mm triangular titanium SI joint implants (SI) following a trans-articular technique [28] (Fig. 2). In total, twenty finite element models were created. Rods and screws were modeled as beam elements with circular cross sections (diameter of 6 mm). Screw shafts were modeled with realistic three-dimensional geometries, whereas screw heads were modeled by means of beam elements and kinematic couplings. The pedicle screws had a diameter of 6.5 mm and a length of 40 mm, the S2AI screws a diameter of 6.5 mm and a length of 65 mm and the iliac screws had a diameter of 7.5 mm and a length of 75 mm. Titanium ($E = 110$ GPa, $\upsilon = 0.3$) material properties were assigned to all implants. The implants were kinematically coupled to bone using the embedded element technique [29], thus assuming the absence of any micromotions.

The intact models were validated by comparing the rotations of the left and right SIJ to in vitro results taken from the literature [30]. Both in vitro tests and numerical simulations were conducted in single-leg stance (i.e., the acetabulum was constrained in all degrees of freedom), and 7.5 Nm was applied to the cranial vertebra in FL-EX, right and left AR, and right and left LB. The ranges of motion (ROM) of the SIJs were calculated as the relative rotation between the sacrum and each ilium.

Following the validations, the treated configurations (IL, S2AI and SI) were investigated and compared to the intact and PED cases. The models were constrained in all

Table 1 Material properties of the ligaments

Ligament	Stiffness (N/mm)	Number of elements	References
Anterior longitudinal	700	3/vertebral body	[24, 25]
Anterior superior iliac	700	10 (×2)	[24, 25]
Posterior short sacroiliac	400	10 (×2)	[24, 25]
Posterior long sacroiliac	1000	4 (×2)	[24, 25]
Pubic	500	10	[26]
Iliolumbar	1000	4 (×2)	[26]
Interosseous	2800	4 (×2)	[24, 25]

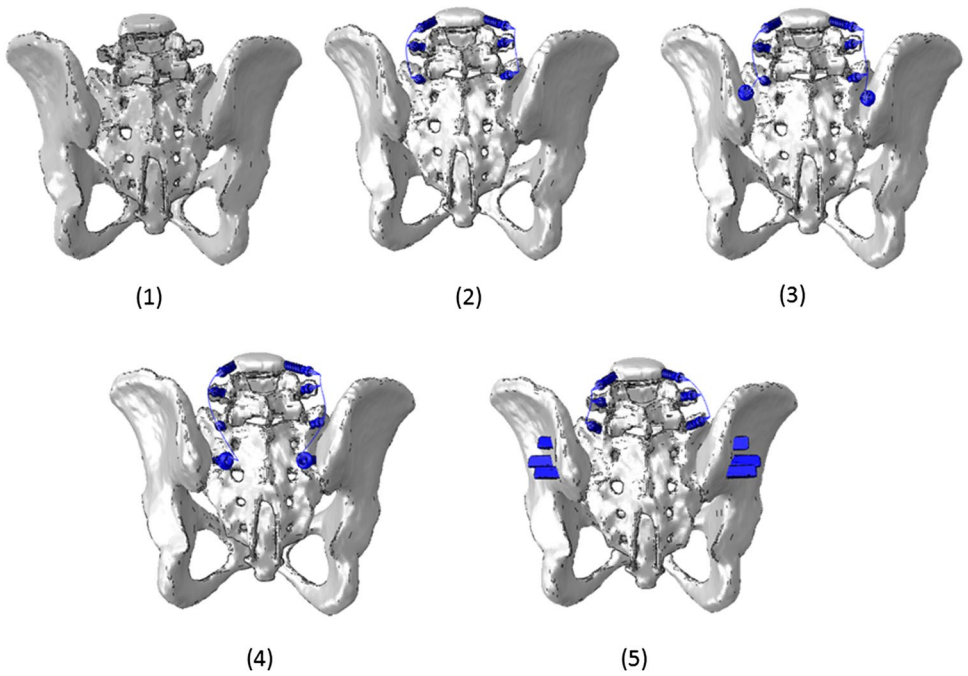

Fig. 2 Lumbosacral configurations investigated: (1) intact, (2) pedicle screws to S1 (PED), (3) pedicle screws to S1 + iliac screws (IL), (4) pedicle screws to S1 + S2AI screws (S2AI), and (5) pedicle screws to S1 + triangular titanium implants (SI)

degrees of freedom at the acetabulum simulating right and left single-leg stance with a 500 N compressive follower load. A 7.5 Nm moment was applied in all motion planes.

The maximum von Mises stresses in the pedicle screws in S1 and in the rods were calculated to estimate which configuration was subjected to the highest risk of failure. For the S1 pedicle screws, the stresses were calculated in the threaded portion, thus excluding the screw heads, whereas in the rods the stresses were calculated for the L5-S1 segment. Since the acetabulum was constrained on one side only, stress values were reported for both the ipsilateral side (IPSI, i.e., rotation on the same side of the constrained acetabulum) and the contralateral side (CONTRA, i.e., on the opposite side). Stresses were reported as median values.

Results

Anatomical reconstruction of the lumbopelvic models

A qualitative comparison of the four models showed the large interindividual difference and variability of the sacropelvic joint documented in the literature [31]. A strong dysmorphic anatomy at the SIJ level was found in Patient 3 (Fig. 3), although the geometrical measurements were in the range defined by the other specimens (Table 2). By the quantitative analysis, the largest differences were found in the PSI of Patient 4 and in the SH of Patient 2 (Table 2).

Validation of the intact model

The range of motion of L5-S1 and of the left and right SIJ were in a good agreement with in vitro measurements [8, 30, 32] (Fig. 4). A large asymmetry in stress data was found in Patient 3 that resulted in outliers during single-leg loading condition, likely due to the strong dysmorphic anatomy at the SIJ level. For this reason, we decided to exclude this patient from the analysis.

Effect of the fixation techniques

In general, all pelvic fixation techniques demonstrated reduced stresses in the S1 pedicle screws with respect to the PED configuration (Table 3). In lateral bending, the absence of pelvic fixation generated stresses up to double those of the other configurations. Among the models including sacropelvic fixation, the highest von Mises stresses in the S1 pedicle screws were found for the IL configuration, followed by SI and S2AI (Table 3). The highest median value was observed in the iliac screw models during flexion (190 MPa), whereas the S2AI and SI models resulted in von Mises median values lower than 160 MPa in any loading condition.

Relative to PED, none of the pelvic fixation techniques had a marked protective effect on the rods in L5-S1. The highest von Mises values were found for IL, with values up to double those of PED. The SI technique was the only configuration that produced rod stresses that were consistently lower than the PED stresses across all motions on the constrained side. In PED, S2AI and SI, von Mises maximum median values were lower than 50 MPa (Table 4). The

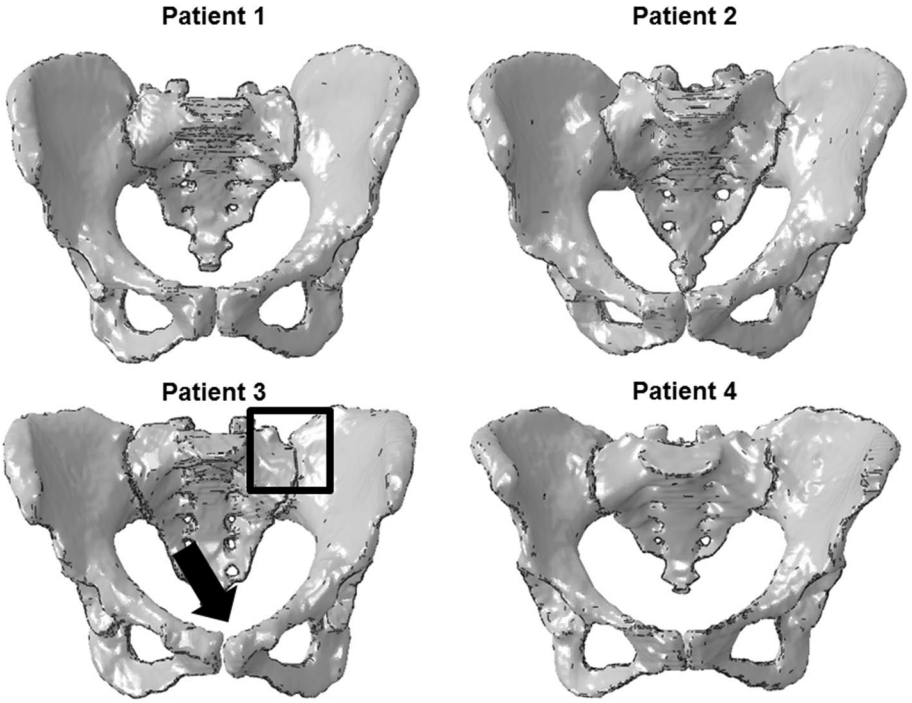

Fig. 3 Reconstructions of the sacropelvic joint of the four female patients involved in the current study. The reconstruction of Patient 3 shows a visible dysmorphia (boxed area) at the SIJ level and at the pubic symphysis (arrow)

Table 2 Anatomical measurements of the four models

	P1	P2	P3	P4
Pelvic sacral incidence (PSI) (deg)	47	56	53	70
Center sacrum to center acetabulum (CS) (mm)	127	138	140	124
Sacral width (mm)	55	41	37	39
Sacral length (mm)	106	110	96	111
S1 length (mm)	44	45	45	50
S1 width (mm)	25	25	24	24
Sacrum height (SH) (mm)	123	167	117	110

highest stresses were in general generated during AR and LB (Table 4).

Discussion

Four finite element models of female patients were generated and validated based on the flexibility of the SIJ [30]. The anatomical reconstruction of the four models shows that Patient 3 had a visible dysmorphia at the SIJ level; because outliers were detected among the von Mises stresses and ROM for the simulations conducted in single-leg stance for this patient, we decided to exclude it from the analysis. However, the anatomical differences among the models support the importance of studying the biomechanics of the SIJ using multiple patient-specific models, instead of one.

This study compared the biomechanical effect of different sacropelvic fixation techniques in terms of von Mises stresses generated in the implants, including a minimally invasive configuration using triangular implants. Nowadays, it is well known that sacropelvic fixation increases the robustness of the construct, with iliac screws and S2 alar-iliac screws being the surgical gold standards. This study revealed that sacropelvic fixation strongly reduces the stresses in S1 pedicle screws but does not have a protective effect on the posterior rods. These findings generally agree with those reported by Hlubek et al. [33], who measured the strain in sacral screws in vitro with and without pelvic fixation with IL, as well with supplementary interbody stabilization at L5-S1. The authors demonstrated that IL fixation was able to significantly reduce the strains in the sacral screws, but increased the strain in the rods at the lumbosacral junction. In addition, we found that fixation by either SI or S2AI similarly reduced von Mises stresses in the S1 pedicles screws and had an equivalent effect on the rods, with clearly better results when compared to iliac screws.

The peak values of von Mises stress in the S1 pedicle screws were in the range found by La Barbera et al. [34, 35] using an ISO model under daily life conditions and lower than the values found using the standard defined in ISO 12189 and ASTM F1717 [36], which replicated a worst case scenario. The peak von Mises stresses in the rods were lower than those in the screws for each configuration. In agreement with La Barbera et al. [34], this result indicates that the pedicle screws are subjected to a higher risk of mechanical failure than the rods. This finding supports previous data

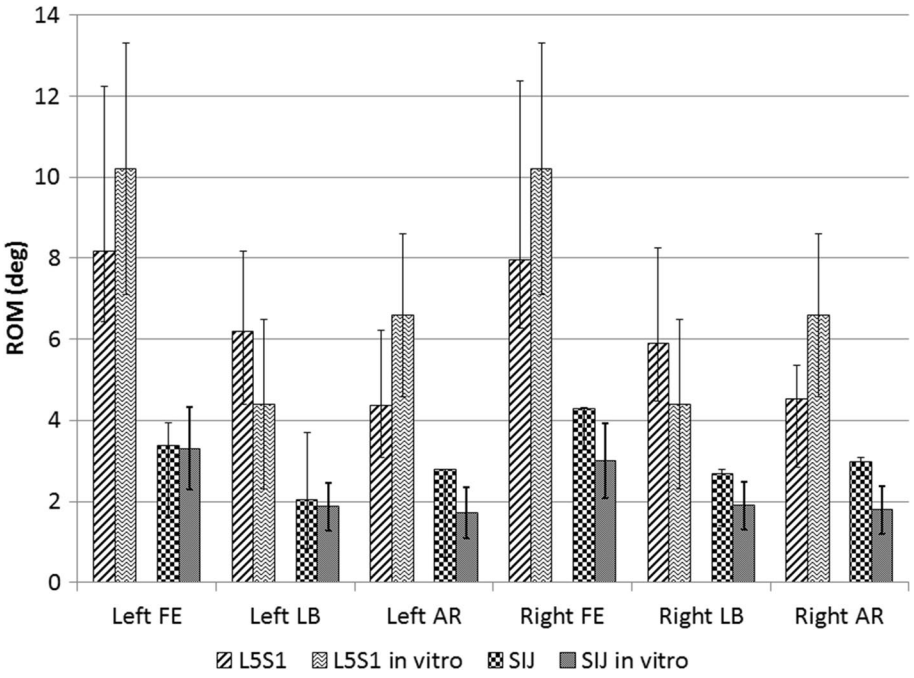

Fig. 4 Median values and minimum–maximum ranges of L5-S1 and of the SIJ for the intact finite element models compared with average and standard deviation of the in vitro results (in vitro results adapted from [8] and [30], respectively). The models and the specimens were constrained in single-leg stance, and 7.5 Nm pure moments in all directions were applied (left/right FE = left/right constrained SIJ flexion extension, left/right LB = left/right constrained lateral bending, left/right AR = left/right constrained axial rotation). L5-S1 in vitro results were obtained in double-leg stance boundary conditions

Table 3 Median values and minimum–maximum range of the maximum von Mises stress (MPa) in pedicle screws in S1

	FL	EX	AR (IPSI)	AR (CONTRA)	LB (IPSI)	LB (CONTRA)
Screw on the constrained side of the model						
PED	213 (84–446)	346 (104–562)	236 (166-685)	149 (98–404)	239 (174–535)	337 (156–476)
IL	190 (134–419)	173 (102–475)	178 (110-315)	121 (55–500)	166 (84–350)	121 (77–410)
S2AI	95 (86–119)	80 (71–125)	119 (108–178)	68 (37–339)	109 (92–206)	120 (65–179)
SI	138 (99–335)	135 (80–182)	111 (61–171)	98 (74–157)	148 (99–236)	110 (64–247)
Screw on the unconstrained side of the model						
PED	226 (150–563)	156 (85–344)	128 (105–332)	236 (166–582)	336 (156-476)	238 (174–535)
IL	163 (45–381)	173 (102–475)	121 (55–500)	178 (110–315)	120 (77–410)	165 (84–350)
S2AI	94 (56–126)	109 (69–179)	67 (37–339)	119 (108–178)	119 (65–179)	124 (92–206)
SI	156 (55–350)	127 (65–163)	90 (64–162)	95 (61–159)	109 (64–247)	148 (99–236)

Table 4 Median values and minimum–maximum ranges of the maximum von Mises stress in rods

	FL	EX	AR (IPSI)	AR (CONTRA)	LB (IPSI)	LB (CONTRA)
Rod on the constrained side of the model						
PED	24 (14–52)	34 (10–52)	31 (17–60)	43 (23–76)	38 (10–68)	29 (19–64)
IL	67 (28–110)	53 (18–64)	74 (29–100)	74 (40–95)	72 (30–97)	47 (23–79)
S2AI	22 (13–40)	26 (10–50)	44 (18–89)	33 (23–75)	48 (24–68)	28 (15–45)
SI	16 (10–44)	20 (12–61)	30 (19–37)	38 (22–69)	30 (12–78)	29 (10–43)
Rod on the unconstrained side of the model						
PED	26 (12–54)	16 (2–29)	25 (20–50)	38 (15–51)	38 (12–63)	32 (17–46)
IL	54 (16–94)	38 (18–73)	59 (29–122)	44 (28–84)	72 (25–99)	64 (18–84)
S2AI	17 (9–45)	28 (10–56)	48 (19–69)	40 (18–59)	20 (7–100)	39 (23–63)
SI	14 (10–43)	21 (10–27)	35 (21–52)	30 (20–84)	31 (10–99)	28 (10–52)

by Pihlajamaki et al. and Chen et al. [37, 38] who studied patients with lumbosacral fixation due to non-traumatic disorders; they reported a lower failure rate in rods than in pedicle screws with the highest rates of screw failure located in the sacrum. However, clinical studies reporting a high rate of rod failure also exist [39].

In this study, the maximum values of stresses generated in the pedicle screws were found in PED configuration, supporting the idea that concomitant pelvic fixation can effectively reduce the S1 pedicle stresses at the lumbosacral level. A similar outcome was found by Sutterlin III and colleagues, which found that S2AI screws reduced the strains in the S1 pedicle screws and in the rods when compared with constructs ending in S1 [8]. Von Mises stresses in S1 pedicle screws were higher after sacroiliac fixation with SI with respect to S2AI, but both techniques resulted in lower stresses when compared with fixation using iliac screws. In the rods, von Mises stresses were found to be the highest in the IL configuration, which may be a result of a posterior load shift. In contrast, S2AI and SI fixation do not have an evident effect on the rod stresses. In summary, S2AI resulted in the lowest risk of S1 pedicle screw failure, whereas the IL configuration seemed to provide no biomechanical advantage in comparison with the other techniques.

This study has some limitations. A simplified loading scenario replicating a single-leg stance in combination with pure moments was employed, whereas complex loads and motions due to the body weight and muscles were not modeled. However, the boundary conditions used were demonstrated to be the worst case scenario for the sacropelvic instrumentation [40] due to the mobility of the pubic symphysis, which moves only marginally when both ilia are constrained, and thus constitute a valuable loading and constraint setting for a comparison between the different techniques. Regarding the fixation techniques, a common solution adopted to increase the stability of the construct and to reduce the stresses on the implants is the insertion of an anterior fixation that has not been investigated in this study. Moreover, only one size for each type of screw was used, as opposed to a range of lengths and diameters, which was selected based on the suggestion of the surgeon investigators.

Another limitation of this study is the lack of S2AI and IL experimental data against which to validate our numerical results; however, we validated the models using ROM data in the intact condition, and the stresses we found in the S1 pedicle screws and rods were in agreement with the literature [8, 30, 41, 42]. Furthermore, we assumed a complete osteointegration of the implants by using the embedded element technique, thus neglecting any effect of possible micromotions at the bone–implant interface, which may increase the ROM of the SIJs and alter the implant and rod stresses. Nevertheless, this modeling choice provided for a direct comparison between the different surgical techniques to investigate the maximum stresses generated in the implants and rods. It should be noted that triangular titanium implants may partly overcome the risk of micromotions and loosening due to the triangular implant shape, spatial disposition along three different planes, and bony ingrowth; further investigation is being performed to better elucidate this issue.

Conclusion

In the current study, a biomechanical comparison between different sacropelvic fixation techniques was performed in terms of stresses in the S1 pedicle screws and in the rods at the L5-S1 level. The study demonstrated that sacropelvic fixation reduces the stresses in the pedicle screws when compared to fixation with pedicle screws only, but none had a protective effect on the rods. Stresses in S1 pedicle screws and rods with S2AI and SI were lower than after fixation with IL, possibly reducing the risk of mechanical failure although the risk of clinical loosening remains an area of further investigation.

Acknowledgements We thank Dr. Enrico Gallazzi for critical reading of the manuscript.

Funding Funding by SI-BONE Inc. (Santa Clara, CA, USA) is gratefully acknowledged.

Compliance with ethical standards

Conflict of interest The authors declare that they have no conflict of interest.

Ethical approval Written informed consent for the use of the data for research purposes was obtained.

References

1. Lombardi JM, Shillingford JN, Lenke LG, Lehman RA (2018) Sacropelvic fixation. When, why, how? Neurosurg Clin North Am 29:389–397. https://doi.org/10.1016/j.nec.2018.02.001
2. Shen FH, Mason JR, Shimer AL, Arlet VM (2013) Pelvic fixation for adult scoliosis. Eur Spine J. https://doi.org/10.1007/s00586-012-2525-3
3. Weistroffer JK, Perra JH, Lonstein JE et al (2008) Complications in long fusions to the sacrum for adult scoliosis: minimum five-year analysis of fifty patients. Spine (Phila Pa 1976) 33:1478–1483. https://doi.org/10.1097/brs.0b013e3181753c53
4. Emami A, Deviren V, Berven S et al (2002) Outcome and complications of long fusions to the sacrum in adult spine deformity: Luque-Galveston, combined iliac and sacral screws, and sacral fixation. Spine (Phila Pa 1976) 27:776–786. https://doi.org/10.1097/00007632-200204010-00017
5. Edwards CC, Bridwell KH, Patel A et al (2004) Long adult deformity fusions to L5 and the sacrum: a matched cohort

analysis. Spine (Phila Pa 1976) 29:1996–2005. https://doi.org/10.1097/01.brs.0000138272.54896.33
6. Fleischer GD, Kim YJ, Ferrara LA et al (2012) Biomechanical analysis of sacral screw strain and range of motion in long posterior spinal fixation constructs: effects of lumbosacral fixation strategies in reducing sacral screw strains. Spine (Phila Pa 1976) 37:7–13. https://doi.org/10.1097/brs.0b013e31822ce9a7
7. Kleck CJ, Illing D, Lindley EM et al (2017) Strain in posterior instrumentation resulted by different combinations of posterior and anterior devices for long spine fusion constructs. Spine Deform 5:27–36. https://doi.org/10.1016/j.jspd.2016.09.045
8. Sutterlin CE III, Field A, Ferrara LA et al (2016) Range of motion, sacral screw and rod strain in long posterior spinal constructs: a biomechanical comparison between S2 alar iliac screws with traditional fixation strategies. J Spine Surg 2:266–276. https://doi.org/10.21037/jss.2016.11.01
9. Kostuik JP (2005) Spinopelvic fixation. Neurol India 53:483–488
10. Kim YJ, Bridwell KH, Lenke LG et al (2006) Pseudarthrosis in long adult spinal deformity instrumentation and fusion to the sacrum: prevalence and risk factor analysis of 144 cases. Spine (Phila Pa 1976) 31:2329–2336. https://doi.org/10.1097/01.brs.0000238968.82799.d9
11. Chang T-L, Sponseller PD, Kebaish KM, Fishman EK (2009) Low profile pelvic fixation: anatomic parameters for sacral alar-iliac fixation versus traditional iliac fixation. Spine (Phila Pa 1976) 34:436–440. https://doi.org/10.1097/brs.0b013e318194128c
12. Daniels AH, DePasse JM, Eltorai AEM, Palumbo MA (2016) Perpendicular iliac screw placement for reinforcement of spinopelvic stabilization. Orthopedics 39:e1209–e1212. https://doi.org/10.3928/01477447-20160729-02
13. Hoernschemeyer DG, Pashuck TD, Pfeiffer FM (2017) Analysis of the s2 alar-iliac screw as compared with the traditional iliac screw: does it increase stability with sacroiliac fixation of the spine? Spine J 17:875–879. https://doi.org/10.1016/j.spinee.2017.02.001
14. Shillingford JN, Laratta JL, Tan LA et al (2018) The free-hand technique for S2-alar-iliac screw placement: a safe and effective method for sacropelvic fixation in adult spinal deformity. J Bone Joint Surg Am 100:334–342. https://doi.org/10.2106/JBJS.17.00052
15. Laratta JL, Shillingford JN, Meredith JS, Lenke LG, Lehman RA, Gum JL (2018) Robotic versus freehand S2 alar iliac fixation: in-depth technical considerations. J Spine Surg 4(3):638–644. https://doi.org/10.21037/jss.2018.06.13
16. Heiney J, Capobianco R, Cher D (2015) A systematic review of minimally invasive sacroiliac joint fusion utilizing a lateral transarticular technique. Int J Spine Surg 9:40
17. Sachs D, Capobianco R (2013) Minimally invasive sacroiliac joint fusion: one-year outcomes in 40 patients. Adv Orthop 2013:536128. https://doi.org/10.1155/2013/536128
18. Bornemann R, Roessler PP, Strauss AC et al (2017) Two-year clinical results of patients with sacroiliac joint syndrome treated by arthrodesis using a triangular implant system. Technol Health Care 25:319–325. https://doi.org/10.3233/THC-161272
19. Schroeder JE, Cunningham ME, Ross T, Boachie-Adjei O (2014) Early results of sacro-iliac joint fixation following long fusion to the sacrum in adult spine deformity. HSS J 10:30–35. https://doi.org/10.1007/s11420-013-9374-4
20. Lindsey D, Kiapour A, Yerby S, Goel V (2015) Sacroiliac joint fusion minimally affects adjacent lumbar segment motion: a finite element study. Int J Spine Surg 9:1–8. https://doi.org/10.14444/2064
21. Lindsey DP, Kiapour A, Yerby SA, Goel VK (2018) Sacroiliac joint stability: finite element analysis of implant number, orientation, and superior implant length. World J Orthop 9:14–23. https://doi.org/10.20959/wjpr2016-6447
22. Le Huec JC, Aunoble S, Philippe L, Nicolas P (2011) Pelvic parameters: origin and significance. Eur Spine J 20(Suppl 5):564–571. https://doi.org/10.1007/s00586-011-1940-1
23. Rho JY, Hobatho MC, Ashman RB (1995) Relations of mechanical properties to density and CT numbers in human bone. Med Eng Phys 17:347–355. https://doi.org/10.1016/1350-4533(95)97314-F
24. Zheng NN, Yong-hing K (1997) Biomechanical modeling of the human sacroiliac joint. Med Biol Eng Comput 35:77. https://doi.org/10.1007/bf02534134
25. Shi D, Wang F, Wang D et al (2014) 3-D finite element analysis of the influence of synovial condition in sacroiliac joint on the load transmission in human pelvic system. Med Eng Phys 36:745–753. https://doi.org/10.1016/j.medengphy.2014.01.002
26. Phillips ATM, Pankaj P, Howie CR et al (2007) Finite element modelling of the pelvis: inclusion of muscular and ligamentous boundary conditions. Med Eng Phys 29:739–748. https://doi.org/10.1016/j.medengphy.2006.08.010
27. Yang H, Jekir MG, Davis MW, Keaveny TM (2016) Effective modulus of the human intervertebral disc and its effect on vertebral bone stress. J Biomech 49(7):1134–1140. https://doi.org/10.1016/j.jbiomech.2016.02.045
28. Soriano-Baron H, Lindsey DP, Rodriguez-Martinez N et al (2015) The effect of implant placement on sacroiliac joint range of motion. Spine 40:E525–E530. https://doi.org/10.1097/brs.0000000000000839
29. Wieding J, Souffrant R, Fritsche A, Mittelmeier W, Bader R (2012) Finite element analysis of osteosynthesis screw fixation in the bone stock: an appropriate method for automatic screw modelling. PLoS ONE 7(3):33776. https://doi.org/10.1371/journal.pone.0033776
30. Lindsey DP, Perez-Orribo L, Rodriguez-Martinez N et al (2014) Evaluation of a minimally invasive procedure for sacroiliac joint fusion:an in vitro biomechanical analysis of initial and cycled properties. Med Devices Evid Res 7:131–137. https://doi.org/10.2147/MDER.S63499
31. Vleeming A, Schuenke MD, Masi AT et al (2012) The sacroiliac joint: an overview of its anatomy, function and potential clinical implications. J Anat 221:537–567. https://doi.org/10.1111/j.1469-7580.2012.01564.x
32. Lindsey DP, Parrish R, Gundanna M et al (2018) Biomechanics of unilateral and bilateral sacroiliac joint stabilization: laboratory investigation. J Neurosurg Spine 28:326–332. https://doi.org/10.3171/2017.7.SPINE17499
33. Hlubek RJ, Godzik J, Newcomb AGUS, Lehrman JN, de Andrada B, Bohl MA, Farber SH, Kelly BP, Turner JD (2018) Iliac screws may not be necessary in long-segment constructs with L5-S1 anterior lumbar interbody fusion: cadaveric study of stability and instrumentation strain. Spine J. https://doi.org/10.1016/j.spinee.2018.11.004
34. La Barbera L, Galbusera F, Wilke HJ, Villa T (2017) Preclinical evaluation of posterior spine stabilization devices: can we compare in vitro and in vivo loads on the instrumentation? Eur Spine J 26:200–209. https://doi.org/10.1007/s00586-016-4766-z
35. La Barbera L, Costa F, Villa T (2016) ISO 12189 standard for the preclinical evaluation of posterior spinal stabilization devices—II: a parametric comparative study. Proc Inst Mech Eng Part H J Eng Med 230:134–144. https://doi.org/10.1177/0954411915621588
36. La Barbera L, Villa T (2016) ISO 12189 standard for the preclinical evaluation of posterior spinal stabilization devices: I—assembly procedure and validation. Proc Inst Mech Eng Part H J Eng Med 230:122–133. https://doi.org/10.1177/0954411915621587
37. Pihlajamaki H, Myllynen P, Bostman O (1997) Complications of transpedicular lumbosacral fixation for non-traumatic disorders. J Bone Joint Surg Br 79:183–189

38. Chen CS, Chen WJ, Cheng CK et al (2005) Failure analysis of broken pedicle screws on spinal instrumentation. Med Eng Phys 27:487–496. https://doi.org/10.1016/j.medengphy.2004.12.007
39. Farrokhi MR, Razmkon A, Maghami Z, Nikoo Z (2010) Inclusion of the fracture level in short segment fixation of thoracolumbar fractures. Eur Spine J 19:1651–1656. https://doi.org/10.1007/s00586-010-1449-z
40. Camisa W, Condez BI, Leasure JM et al (2014) Development of a biomechanical model for sacroiliac range of motion. In: 2014 AAOS Annual Meeting, pp 42–43
41. Ambati D, Wright E, Lehman R et al (2015) Bilateral pedicle screw fixation provides superior biomechanical stability in transforaminal lumbar interbody fusion: a finite element study. Spine J 15(8):1812–1822
42. Liu C, Kamara A, Yan Y (2018) Investigation into the biomechanics of lumbar spine micro-dynamic pedicle screw. BMC Musculoskelet Disord 19(231):1–11

Affiliations

Gloria Casaroli[1] · Fabio Galbusera[1] · Ruchi Chande[2] · Derek Lindsey[2] · Ali Mesiwala[3] · Scott Yerby[2] · Marco Brayda-Bruno[1]

✉ Fabio Galbusera
fabio.galbusera@grupposandonato.it

Gloria Casaroli
gloria.casaroli@grupposandonato.it

Ruchi Chande
rchande@si-bone.com

Derek Lindsey
dlindsey@si-bone.com

Ali Mesiwala
amesiwalamd@gmail.com

Scott Yerby
syerby@si-bone.com

Marco Brayda-Bruno
marco.brayda@spinecaregroup.it

[1] IRCCS Istituto Ortopedico Galeazzi, Milan, Italy

[2] SI-BONE, Inc., San Jose, CA, USA

[3] Southern California Center for Neuroscience and Spine, Pomona, CA, USA